CSIRO PUBLISHING

Aust. J. Chem.
https://doi.org/10.1071/CH18447

Full Paper

Preparation and Characterization of a PVDF Membrane Modified by an Ionic Liquid

Pengzhi Bei,[A] *Hongjing Liu,*[A,B] *Hui Yao,*[A] *Yang Jiao,*[A] *Yuanyuan Wang,*[A] *and Liying Guo*[A]

[A]School of Petrochemical Engineering, Shenyang University of Technology, Liaoyang 111003, China.
[B]Corresponding author. Email: liuhongjing_101@126.com

In order to enhance the hydrophobicity of polyvinylidene fluoride (PVDF) porous membranes, the blending of PVDF with a hydrophobic ionic liquid (IL) 1-butyl-3-methylimidazolium hexafluorophosphate ([Bmim][PF_6]) was carried out. The modified PVDF membranes with [Bmim][PF_6] were fabricated through a non-solvent induced phase inversion using lithium chloride as a porogen in the PVDF casting solution. The effects of [Bmim][PF_6] on the membrane characteristics were investigated. FT-IR analysis indicates that the IL is successfully retained by the PVDF membrane. Thermogravimetric analysis reveals that the optimum temperature of the modified membrane is below 300°C. Scanning electron microscopy pictures show that modified membranes have more homogeneous and larger diameter pores with a mean pore size of 0.521 μm and porosity of 78 %. By measuring the IL leaching during the membrane fabrication, it was found that the modified membrane does not lose IL. Atomic force microscopy shows that the roughness of the modified membrane surface increases slightly, but the contact angle of the modified membrane increases significantly from 88.1° to 110.1°. The reason for this is that the fluorine-containing IL has a low surface energy, which can enhance the hydrophobicity of the membrane. Finally, by comparing modified membranes with different IL concentrations, we draw a conclusion that the modified membrane with an IL concentration of 3 wt-% has the best properties of pore size, porosity, and hydrophobicity.

Manuscript received: 6 September 2018.
Manuscript accepted: 11 February 2019.
Published online: 15 March 2019.

Introduction

In recent years, the development of membrane absorption technology has become more advanced, with the potential to overcome the disadvantages of conventional gas absorption equipment such as high energy requirements for regeneration and thermal degradation.[1–3] CO_2 capture using membrane contactors combines chemical absorption and membrane separation processes.[4–7] However, this method also has its own disadvantages, namely, an additional mass transfer resistance due to the addition of the membrane itself.[8] If the membranes have low hydrophobicity and they are easily wetted by the solution, the membrane resistance becomes particularly high, and the occurrence of this phenomenon is extremely unfavourable for the absorption of CO_2. As such hydrophobic membranes play an important role in the CO_2 absorption of membrane contactors.[9] Alternatively, membrane distillation (MD) is a highly efficient membrane separation process which is needed to avoid wetting by a highly hydrophobic or low surface energy membrane. The increase of hydrophobicity will lead to the improvement of performance in membrane distillation.[10,11]

Hydrophobic membranes such as polypropylene (PP), polyethylene (PE), polytetrafluorethylene (PTFE), and polyvinylidene fluoride (PVDF) are currently the most widely used polymeric materials.[12] However, the fluorine-containing polymeric membranes are more hydrophobic than PP and PE.[13] Although PTFE has a strong hydrophobicity, its application is limited due to its high price.[14] Microporous PVDF membranes are some of the most promising candidates for use in membrane contactors because of their relatively high hydrophobicity, chemical resistance, and reasonable material cost. PVDF is an important polymer with a repeat unit of $–(CH_2CF_2)_n–$, and has been applied in industry, especially in separation membranes, owing to its high mechanical strength, high thermal stability, excellent aging resistance, as well as good chemical resistance.[15] Many papers have been published about PVDF modification. Rezaei et al.[16] used a PVDF/montmorillonite (MMT) mixed membrane to absorb CO_2. The results showed that the absorption efficiency is better, and the hydrophobicity of the mixed membranes is higher than that of commercial membranes. Rahbari-Sisakht et al.[17] fabricated a novel surface modified PVDF hollow fibre membrane by adding a surface modifying macromolecule as an additive in a spinning dope. Their results indicate that the modified PVDF membrane has a higher performance due to the improvement in pore size, higher effective surface porosity, as well as the increased hydrophobicity of the membrane surface. Zhang et al.[18] prepared a composite membrane with a ZrO_2 solid superacid shell/void/TiO_2 (ZVT). The results indicate that anti-fouling, anti-compaction, and hydrophilicity are enhanced. They thought that ZVT was a desirable functional nanomaterial due to the presence of microreaction locations (MRL) inside the channels of PVDF.

An effective method to change the hydrophobicity of a membrane surface is to introduce some additives into the casting solution to modify the surface energy. Since fluorine-containing materials have a low surface energy, they tend to reduce the interaction between the membrane surface and the absorbent so as to increase the hydrophobicity. Razmjou et al.[19] prepared a super-hydrophobic PVDF membrane with a water contact angle of 163°. The super-hydrophobicity was a result of a titania coating which provided a hierarchical structure and site for functionalization. Park et al.[20] developed fluorine-containing thermally rearranged nanofiber membranes (F-TR-NFMs) for MD applications for the first time. F-TR-NFMs had enhanced hydrophobic properties with a high water contact angle (143°) and excellent energy efficiency according to their experimental results.

The development of ionic liquids (ILs) is currently a topic of great interest for researchers and they are one of the promising compounds for CO_2 gas recovery.[21] ILs are special salts composed of organic cations and inorganic anions, and they exist in the liquid phase with negligible vapour pressure at room temperature.[22–24] ILs have other excellent characteristics such as good thermal stability, and high ionic conductivity and solubility in organic media.[25] In recent years, ILs have been widely used to modify membrane materials because of their excellent properties, which has attracted the attention of many scholars. The application of hydrophobic ILs to modify polymer membranes is widely used. Imidazolium-based ILs have been chosen because their physical and chemical properties are more stable in comparison to other ILs.[26] In particular, 1-butyl-3-methylimidazolium hexafluorophosphate ([Bmim][PF_6]) has been used in membrane applications in several articles. Lakshmi et al.[27] obtained hydrophilic porous polyethersulfone (PES) membranes with [Bmim][PF_6] and applied the new membranes to remove reactive blue 19 (RB19). They found that the optimum conditions for membrane preparation are as follows: [Bmim][PF_6] concentration 10.7 wt-%, membrane weight 0.055 mg, pH 3.0, and dye concentration 10.0 ppm. Mahdavi et al.[28] synthesised polyether-*block*-amide (Pebax1074) using [Bmim][PF_6] and silica nanoparticles in order to separate carbon dioxide and methane. The results show that [Bmim][PF_6] can improve the solubility of CO_2, so the CO_2 permeability increases from 58.6 to 104.3 Barrer at a [Bmim][PF_6] concentration of 80 wt-%. Akhmetshina et al.[29] prepared supported ionic liquid membranes (SILMs) using [Bmim][PF_6] and [emim][NTf_2] (1-ethyl-3-methylimidazolium bis[(trifluoromethyl)sulfonyl]imide) to separate mixed gases. They found that ILs can be immobilized into the pores of the polymer. Their experimental results show that the ideal selectivity of the modified membranes has interesting prospects. Chaurasia et al.[30] studied the effect of [Bmim][PF_6] on the crystallization behaviour of poly(ethylene oxide) (PEO). The experimental results indicate that [Bmim][PF_6] can slow down the rate of crystallization of PEO membranes. In addition, ILs containing fluorine have attracted much attention. Lin et al.[31] successfully synthesized and characterized phosphoric acid doped hydrophobic IL based composite membranes. 1-Vinyl-3-butylimidazoliumbis(trifluoromethylsulfonyl)-imide ([VBIm][NTf_2]) was synthesized and used as hydrophobic phase in composite membranes. The resultant composite membranes showed good thermal stability and mechanical properties, and high proton conductivity. Awasthi et al.[32] synthesized nanophase-separated poly(arylene ether) multiblock copolymers and obtained the membranes with 1-butyl-3-methyl-imidazolium tetrafluoroborate by a solution casting method, which exhibited good dimensional and thermal stability. The complexation of the multiblock copolymer resulted in novel hybrid membranes.

Fluorinated membranes have significant importance in separation due to their inertness and fouling resistance. Al-Gharabli et al.[33] developed a novel modification methodology of PVDF membranes employing piranha reagent to activate the fluorinated surface followed by consecutive grafting with H^1,H^1,H^2, H^2-perfluorooctyltriethoxysilane (FC_6). A higher roughness and contact angle and more open structure were noticed in comparison to the pristine membrane. An improvement of mechanical features was also observed for the membrane functionalized by FC_6. Saiz et al.[34] compared the effects of three different ILs diethylmethylammonium trifluoromethanesulfonate ([dema][TfO]), 1-methylimidazolium bis(trifluoromethylsulfonyl)imide ([Mlm][NTf_2]), and 1-methylimidazolium chloride ([Mlm][Cl]) on poly(vinylidene fluoride-co-hexafluoropropylene) (PVDF-HFP) membrane properties under various preparation conditions. They found that the pore size and resultant hydrophobicity depended on the production method and the types of ILs.

It can be seen from previous research that the influence of fluorine on hydrophobicity is very important. Nowadays, polyfluorinated inorganic anions are numerous, such as NTf_2 and PF_6, and they are the most commonly used in ILs.[35] These anions impart a much higher hydrophobicity and better functionality than other conventional fluorinated anions. However, the preparation of a modified PVDF membrane blended with [Bmim][PF_6] to improve membrane hydrophobicity has not been reported. Therefore, we prepared PVDF membranes blended with different concentrations of [Bmim][PF_6] in this work. The modified membranes were characterized by FT-IR, differential scanning calorimetry (DSC), thermogravimetric analysis (TGA), scanning electron microscopy (SEM), and atomic force microscopy (AFM). Measurements of the modified membranes were carried out in terms of pore size, porosity, IL leaching, and hydrophobicity.

Experimental

Materials

PVDF powder (FR-904, $\sim 1.02 \times 10^6$ g mol^{-1}) was purchased from Shanghai 3F New Materials Technology Co., Ltd, China. *N*,*N*-Dimethylformamide (DMF) was provided by Tianjin Guangfu Fine Chemical Research Institute, China. [Bmim][PF_6] was obtained from Shanghai Cheng Jie Chemical Co., Ltd, China. Lithium chloride was provided by Beijing Beihua Fine Chemicals Co., Ltd, China.

Preparation of PVDF Membrane Modified by IL

A PVDF microporous membrane was prepared by an immersion precipitation method with 3 wt-% LiCl as additive and DMF as solvent. [Bmim][PF_6] at different concentrations was added to the casting solution for blending. The casting solution was stirred for 4 h at 60°C until the PVDF powder had been completely dissolved in DMF. The homogenous casting solution obtained was left to stand for 24 h for deaeration. The casting solution was then cast onto a clean glass plate after the bubbles had been removed. Immediately, the glass plate was horizontally immersed in deionized water at 4°C for at least 24 h so that a solid membrane was prepared and was tested after removal of the solvent.

Table 1. Compositions of the modified membranes with different IL concentrations

Membrane	PVDF [wt-%]	LiCl [wt-%]	[Bmim][PF_6] [wt-%]	DMF [wt-%]
IL-0wt%	15	3	0	82
IL-2wt%	15	3	2	82
IL-3wt%	15	3	3	82
IL-4wt%	15	3	4	82

The compositions of the modified membranes with different IL concentrations are presented in Table 1.

Characterization of the Modified Membrane

FT-IR spectrometry (Thermo Nicolet Corporation NEXUS-470, USA) was applied to detect the membrane surface groups qualitatively with a wavenumber range of 400–4000 cm^{-1}. SEM (Japan Hitachi Nake high-tech enterprise, TM300) was used to observe the cross-section morphology of the membrane. DSC (Mettler Toledo DSC-822e, Switzerland) was used to characterize the melting point and crystallization kinetics process of the modified membrane. TGA was performed using a TGA 4000 (PerkinElmer, USA) with a N_2 atmosphere from 25–800°C and a heating rate of 10°C min^{-1} to confirm the thermal properties of each membrane. The contact angle of the membrane surface was measured using a contact angle analyzer (Beijing Dongfang Defei Instrument Co., Ltd, China), measurements were performed at least 10 times to ensure the reproducibility of measurement results. The viscosity of the prepared casting solution was measured by viscometry (EW-98965-40, Cole-parmer, USA). The surface roughness of the prepared membranes was examined using AFM (Bioscope Catalyst Atomic Force Microscopy, Bruker Corporation, USA). The IL loss was measured by a conductivity meter (Shanghai INESA Scientific Instrument Co., Ltd, China).

Measurement of Pore Size of the Modified Membrane

The measurement of pore size of the modified membrane was done by a gas permeation test. By assuming cylindrical pores in the skin layer of the asymmetric membranes, the gas permeance can be calculated as follows:[36]

$$J_A = \frac{2r_p\varepsilon}{3rTL_p}\left(\frac{8RT}{\pi M}\right)^{0.5} + \frac{r_p^2\varepsilon}{8\mu RTL_p}\bar{P} \qquad J_A = K_0 + P_0\bar{P} \quad (1)$$

where J_A is the gas permeance (mol m^{-2} s^{-1} Pa^{-1}), r_p and L_p are the pore radius and effective pore length, respectively (m), ε is the surface porosity, R is the gas constant (8.314 J mol^{-1} K^{-1}), μ is the gas viscosity (kg m^{-1} s^{-1}), M is the gas molecular weight, T is the gas temperature (K), and $\bar{P}$ is the mean pressure (Pa).

By plotting J_A with mean pressures according to Eqn 1, the mean pore size can be determined (Eqn 2):

$$r_p = 5.333\left(\frac{P_0}{K_0}\right)\left(\frac{8RT}{\pi M}\right)\mu \quad (2)$$

The dry membrane was cut into a circular shape and placed in the membrane cell. After checking the air-tightness of the device, the gas flow rate was recorded under different pressures until the gas flow into the membrane cell was stable. Finally, the gas permeation flux was calculated by the formula as described above. Pure N_2 was used as the test gas. The flowsheet for the test of gas permeation flux is shown in Fig. 1.

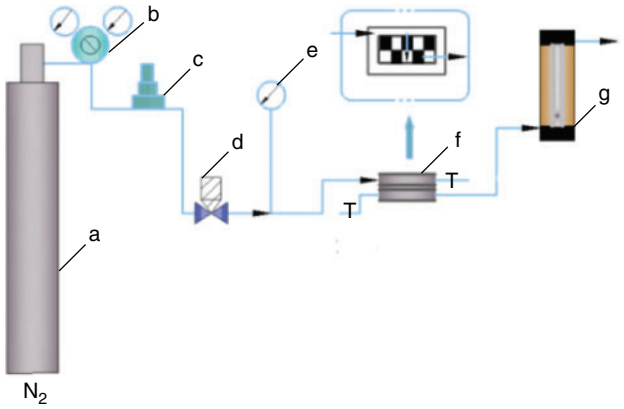

Fig. 1. Flowsheet for testing gas permeation flux. (a) Nitrogen cylinder, (b) pressure gauge, (c) constant pressure, (d) control valve, (e) digit-display manometer, (f) membrane module, (g) rotameter.

Measurement of Porosity of the Modified Membrane

The membranes were weighed as wet membranes before being dried in an oven to eliminate any moisture. The dry membranes were also weighed in order to calculate the porosity using the following equation:

$$\varepsilon = \frac{m_n/\rho_n}{m_n/\rho_n + m_p/\rho_n} \times 100\,\% \quad (3)$$

where ε is the porosity of the membrane, m_p is the mass of the dry membrane (g), m_n is the mass of the absorbed water (g), ρ_p is the density of the PVDF (1.805 kg cm^{-3}), and ρ_n is the density of water (1.0 kg cm^{-3}).

In this calculation, a total of five measurements were taken based on five different locations within the same membrane sample and the average value was taken, which ensured that the porosity test covered the whole membrane surface.

Measurement of Critical Water Inlet Pressure of the Modified Membrane

An ultrafiltration cup (SCM300; Ecologic Center China) was used to measure the membrane permeability, in which the effective filtering area of the membrane was 33.2 cm^2. The experiment was carried out at 25°C and 100 kPa.

The wet membrane was cut into a circular shape and placed in the ultrafiltration cup. In the flux measurement, it was necessary to precompact each membrane with deionized water at 150 kPa until the flux reached a stable value. The flow sheet for determining the critical water inlet pressure is shown in Fig. 2.

Determination of IL Leaching of the Modified PVDF Membrane

The IL has a certain electrical conductivity in water, and this characteristic is used to measure the IL-leaching rate of the modified PVDF membrane.

We measured the conductivity of three casting solutions which contained 2, 3, and 4 wt-% of IL, respectively. After

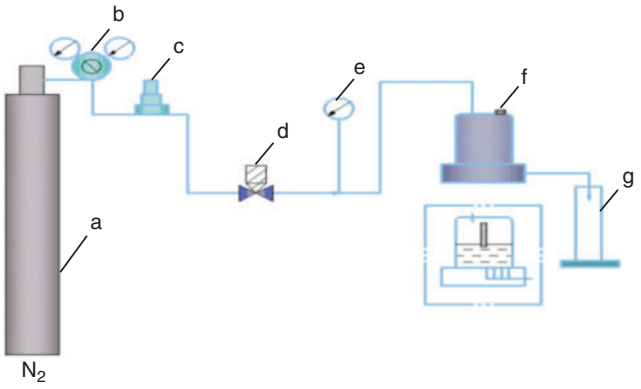

Fig. 2. Experimental set up for determining theoretical water inlet pressure. (a) Nitrogen cylinder, (b) pressure gauge, (c) constant pressure, (d) control valve, (e) digit-display manometer, (f) ultrafiltration cup, (g) cylinder.

putting the membrane into 100 mL of the deionized water, the conductivity of the deionized water immersed modified membrane was measured and sampled every 2 h at 25°C for 10 days, and finally the IL-leaching rate β determined. β was calculated by Eqn 4:

$$\beta = \frac{\mu_t}{\mu_0} \times 100\,\% \tag{4}$$

where μ_0 (μs cm^{-1}) is the initial conductivity of deionized water and μ_t (μs cm^{-1}) is the conductivity of deionized water at the time of measurement.

Results and Discussion

FT-IR Analysis of the Modified Membrane

FT-IR analysis was performed to confirm whether [Bmim][PF_6] was successfully left in the modified membrane. The spectra of the unmodified and modified PVDF membranes are illustrated in Fig. 3.

As shown in Fig. 3, the modified membrane has wide absorption peaks at 3125.13, 1577.93, and 841.7 cm^{-1}. The peak at 3125.13 cm^{-1} can be attributed to the stretching vibration of the IL imidazole C–H ring. The absorption peak at 1577.93 cm^{-1} corresponds to the band adsorption of the heterocyclic imidazolium ring covalently anchored on the polymer support.[37,38] The peak at 841.71 cm^{-1} is the typical stretching vibration of P–F.[39] The peak at 832.07 cm^{-1} is the C–H characteristic peak of PVDF.[40] Because the IL content is poor, the peak area of 841.17 cm^{-1} is small, however the peaks shown in Fig. 3 are enough to confirm the presence of [Bmim][PF_6] in the membrane.

Thermal Properties Analysis (DSC)

DSC analysis of the PVDF and modified PVDF membranes was conducted to examine the effect of [Bmim][PF_6] on the melting point and degree of crystallinity of the membranes. The DSC curves are presented in Fig. 4. It is observed that the pristine membrane shows an endothermic melting peak at 163.95°C and the modified membrane shows an endothermic melting peak at 166.57°C. We can see that the melting point of the modified membrane is lower than that of the pristine membrane. This indicates that the formation of a mixture will lower the melting point.

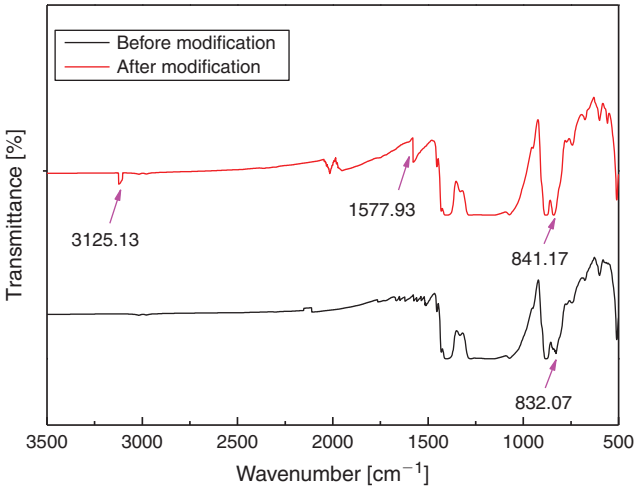

Fig. 3. FT-IR spectra of modified and unmodified membranes.

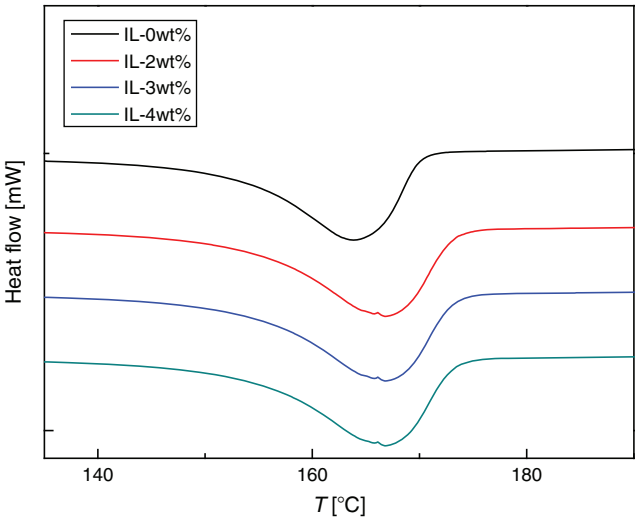

Fig. 4. DSC curves of PVDF membranes with different IL concentrations.

Both pristine and modified membranes show an exothermic crystallization peak at around 135°C as shown in Fig. 5, which verifies that the [Bmim][PF_6] has no significant influence on the crystallization of PVDF. The reason is that the addition of IL does not destroy PVDF symmetry within the concentration range of the experiment.

Thermogravimetric Analysis (TGA)

Thermal stability is a significant property for the practical application of modified membranes in various applications, which can further influence the process of membrane absorption. In this regard, the determination of the stability of the modified membrane is valuable.[41]

In this study, the thermal stability of the pristine and modified membrane was determined by TGA and the results obtained are shown in Fig. 6. We examined the TGA curve of the pristine membrane. First, due to its moisture sensitivity a slight weight loss was observed above 450°C. Second, we can clearly observe that a decomposition process occurred between 450 and 510°C, attributable to the decomposition of PVDF. The main chain pyrolysis of PVDF occurs at ~450°C with the evolution of HF.

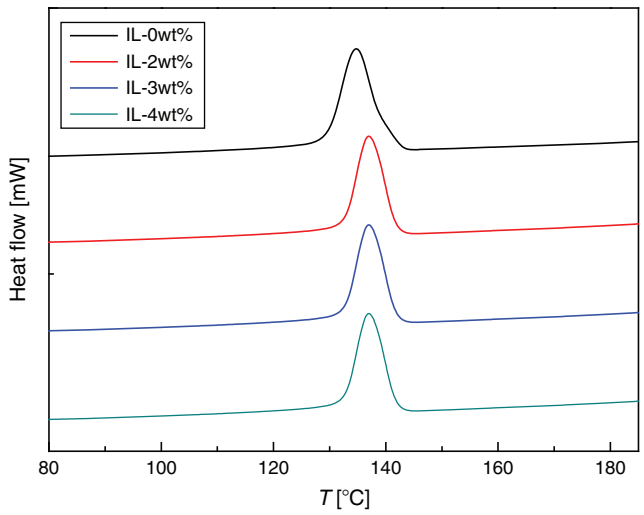

Fig. 5. DSC endotherm curves of PVDF membranes with different IL concentrations.

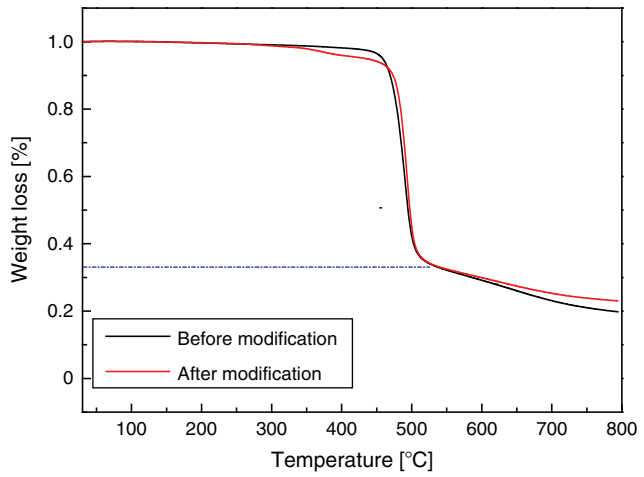

Fig. 6. TGA curves of the prepared membranes.

The pristine membrane lost ~62 % weight at 510°C. The theoretical loss should be 62.5 %, which is almost identical to the TGA image, indicating that only the C skeleton remains after 510°C.

In comparison to the pristine membrane, the TGA curve of the modified membrane first underwent a slight weight loss at 300°C due to its moisture sensitivity. Second, the modified membrane started to decompose at 300°C, this weight loss is attributed to the loss of the ILs anchored on the polymer support and ended at 470°C. The modified membrane lost ~10 % at 470°C. The theoretical loss of IL was calculated to be 14 % which is in good agreement to the TGA image, confirming that that IL has been lost from the membrane. Third, the largest weight loss was initiated at 470°C where the decomposition of the polymer backbone chain occurred and only the C skeleton remained at 510°C just like the pristine membrane. In summary, the modified membrane shows an important two-step degradation pattern as shown in Fig. 6. The first step is attributed to the decomposition of the ILs, and the second step mainly reflects the decomposition of the polymer chain.[42]

From the TGA curve, we can conclude that the optimum temperature of the modified membrane should be below 300°C

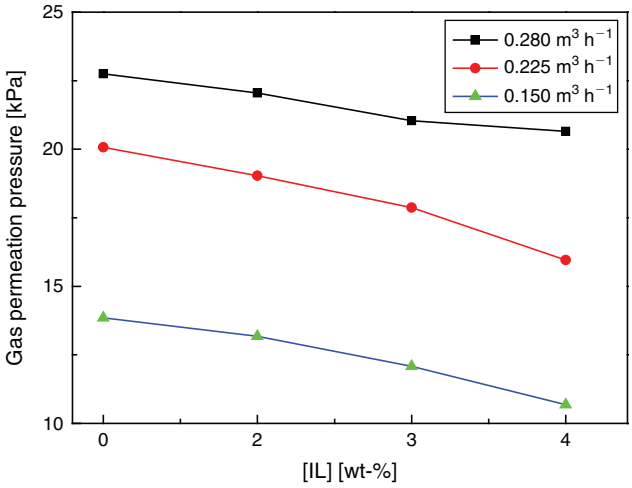

Fig. 7. Change of gas permeation pressure with IL concentration of PVDF membranes.

in order for the ILs to play a role in the membranes function and the thermal stability of the PVDF is not affected by the addition of IL.

Structure

A gas permeation test was used to measure the mean pore size of the fabricated membranes quantitatively. The relationship between gas permeation pressure and IL concentration in the modified membranes is shown in Fig. 7 at three gas flow rates: 0.15, 0.225, and 0.280 $m^3\ h^{-1}$. We can see that the gas permeation pressure of the modified membrane decreases for the modified membrane compared with the pristine membrane (IL-0wt%). As the content of the IL increases, the gas permeation pressure of the IL modified membrane gradually decreases. The change implies that the membrane pore structures are different. The calculated pore size and porosity of the membranes are shown in Table 2.

PVDF being a polymer was precipitated to prepare membranes by liquid–liquid demixing during the course of immersion precipitation.[43] The mechanism of pore formation for the PVDF membrane is very complicated. Many scholars have explored the pore-forming mechanism of these membranes since 1972.[44–47] It is now generally accepted that liquid–liquid demixing by means of nucleation and growth of the diluted phase is the pore forming mechanism during membrane formation. From this mechanism, we can see that the instantaneous type phase separation and the delayed type phase separation can form different pore size structures. Instantaneous type phase separation leads to large pores and delayed type phase separation gives rise to small pores. According to the mechanism mentioned above, when the rate of water entering the film is faster than that of the solvent leaving, larger pores and more porous membranes will be formed during the precipitation. Otherwise, small pores will be formed.[48] Generally, the porosity and pore size of polymeric membranes are dependent on each other, and an increasing pore size tends to enhance porosity.[49]

In this experiment, we prepared modified membranes with DMF as the solvent and IL as the additive. The addition of ILs can affect the phase separation from two aspects and provide two competitive processes. On the one hand, the H of C–H between two nitrogen atoms in the imidazole ring can form hydrogen bonds during casting with the C=O of DMF as shown

Table 2. Characteristics of the PVDF membranes with different IL concentrations

Membrane	Mean pore size [μm]	Porosity [%]	Solution casting viscosity [cP]	Contact angle [deg.]	Inlet pressure [kPa]
IL-0wt%	0.194 ± 0.02	71 ± 0.73	1129	88.1 ± 2.1	96
IL-2wt%	1.74 ± 0.03	74 ± 0.68	1135	97.2 ± 1.4	108
IL-3wt%	0.521 ± 0.04	78 ± 0.75	1290	110.1 ± 1.8	172
IL-4wt%	1.41 ± 0.02	70 ± 0.81	1340	96.9 ± 2.0	150

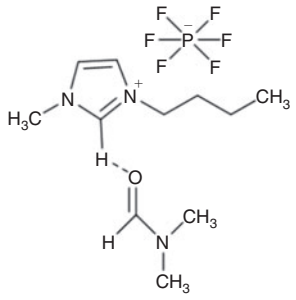

Fig. 8. Hydrogen bonding interaction between [Bmim][PF_6] and DMF.

in Fig. 8. Therefore, the presence of hydrogen bonds can slow the rate at which DMF leaves the membrane, which results in the formation of large pore sizes.[43] On the other hand, the IL has the characteristic of high viscosity.[50] The viscosity of the casting solution can increase with the increase of IL content as shown in Table 2. The increase of viscosity can promote the delayed type phase separation, which is suitable for the formation of small pores. In summary, large pores are formed by instantaneous type phase separation, and small holes are formed by delayed type phase separation, so the pore size and porosity is determined by the two competitive processes as mentioned above.

From Table 2, it can be seen that the pore size and porosity of the modified membrane are improved to some extent compared with the pristine membrane. The mean pore size of the modified membranes is larger than that of the pristine membrane, indicating that the effect of the hydrogen bonding between the IL and DMF is more significant than that of viscosity. However, membranes with different concentrations of IL have different effects on membrane structure as shown in Table 2. The modified membrane with an IL concentration of 2 wt-% has the maximum mean pore size. The reason for this is that the hydrogen bond between the IL and DMF dominates the relative rate at which water enters and the solvent leaves the casting solution, so that large pores are formed. The pore size of the modified membrane with an IL concentration of 3 wt-% is smaller than the other two modified membranes (IL-2wt% and IL-4wt%), but the porosity is the largest. In this case, although the action of hydrogen bonding is still stronger than the effect of viscosity, the competitiveness of the hydrogen bonding becomes relatively weak due to the obvious increase in solution viscosity. However, when 4 wt-% IL is added, the pore size increases again and the porosity becomes minimal, indicating that hydrogen bonding can be enhanced due to the higher content of IL, which aggravates the instantaneous type phase separation to form larger pores. By comparing the modified membranes, it can be seen that IL-3wt% has the smallest mean pore size and largest porosity among the modified membranes, which makes the pores of the membrane more evenly distributed and has the best structure of the modified membranes.

The morphology of the prepared PVDF membranes was examined by SEM. All of the membranes showed a typical asymmetrical structure. The pristine membrane has two layers: the sponge-like upper layer and the slanting finger-like bottom layer as shown in Fig. 9a. The modified membranes have more finger-like pores and less sponge-like pores. The observation indicates that modified membranes have pronounced changes in the pore morphology with more well distributed voids and a larger diameter. It is well known that the solvent–non-solvent exchange rate during phase inversion controls the structure of asymmetric membranes.[51] From the SEM images of the modified membranes, it can be seen that the modified membrane with an IL concentration of 3 wt-% has a better finger-like structure and uniform pores throughout the cross-section as shown in Fig. 9c. The modified membranes of IL-2wt% and IL-4wt% have similar finger-like macrovoids in the cross-section, indicating a heterogeneous distribution of pores and the pore size, as shown in Fig. 9b, d. These SEM figures agree with our experimental results as well as our analysis about pore size and porosity as mentioned above.

Contact Angle

Hydrophobicity is an important property of PVDF membranes. The hydrophobicity of the membranes was characterized through water contact angle measurement. The values are listed in Table 2 and photos of contact angles are shown in Fig. 9. Overall, the contact angles are in the range of 96.6°–110.1°, which indicates an improved hydrophobicity of the membrane compared with a previous study.[52] [Bmim][PF_6] contains fluorine which is the most electronegative element. This strong electronegativity increases the affinity of F and C, making the bond energy of C–F much larger than that of C–H. The stability of the fluorine-containing substance is obviously enhanced, so the fluorine-containing IL has the characteristics of low surface energy. Adding the fluorine-containing IL to the casting solution will reduce the surface energy of the modified membranes, which leads to a higher hydrophobicity.

On the other hand, compared with the other two modified membranes (IL-2wt% and IL-4wt%), the modified membrane prepared with IL-3wt% has the largest contact angles, namely 110.1°. The higher IL concentration (IL-4wt%) does not lead to a higher contact angle. The reason is that excessive fluorine (4 wt-%) can bind carbon more firmly and can cause two competing processes between the exterior and interior of the membrane. When the concentration of fluorine is increased to a certain extent, the action of fluorine and hydrogen can reduce the action of C–F on the surface of the membrane, resulting in an increase of hydrophilicity. So the hydrophobicity of the surface is not significantly increased. In general, the higher the hydrophobicity, the higher the critical inlet pressure. From Table 2, we

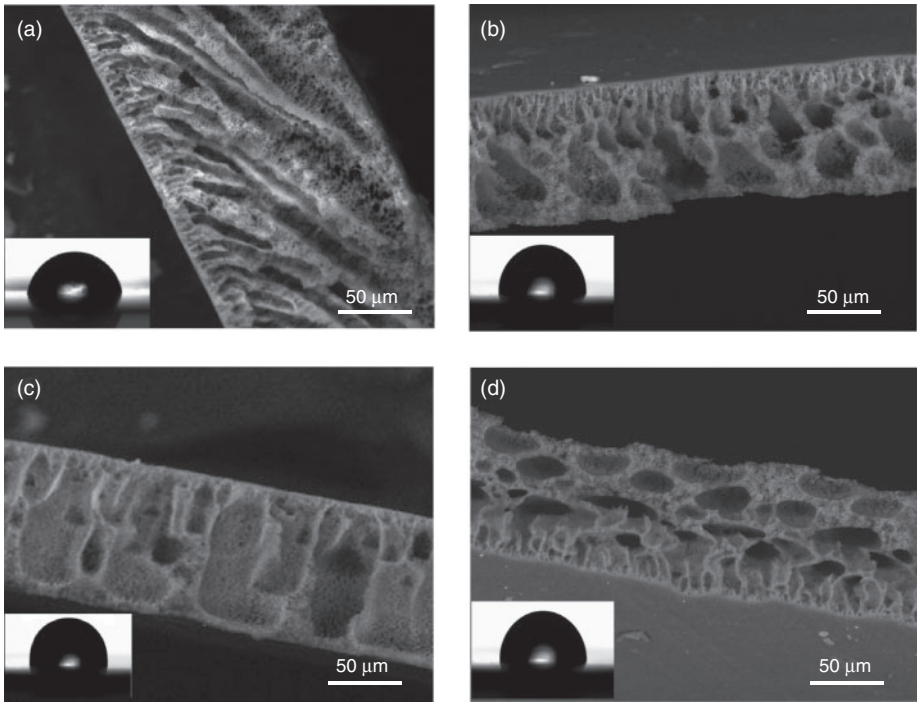

Fig. 9. SEM and contact angle images of membranes with different IL concentrations: (a) IL-0wt% (b) IL-2wt% (c) IL-3wt%, and (d) IL-4wt%.

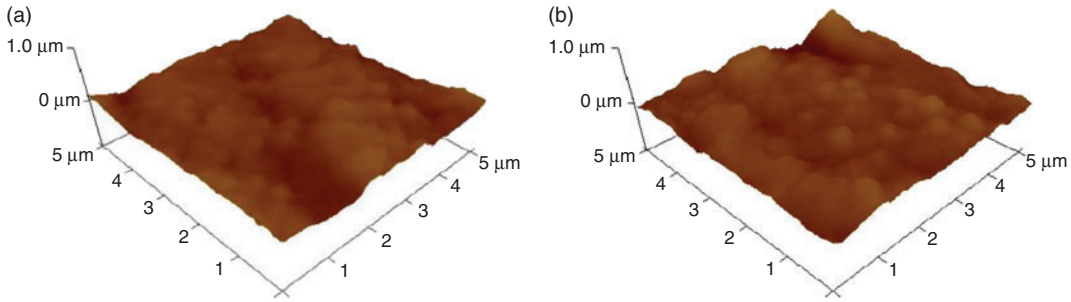

Fig. 10. AFM of pristine and modified membrane (IL-3wt%). (a) Pristine membrane (Ra = 46.3 nm, Rq = 59.2 nm). (b) Modified membrane (Ra = 47.1 nm, Rq = 62.2 nm).

can see that the membrane with 3 wt-% IL concentration has the highest critical inlet pressure, whose changing trend is in agreement with that of the contact angle.

The hydrophobicity of a membrane is generally determined by the surface energy and roughness of the membrane surface. Accordingly, AFM was used to visualise the surface of the pristine membrane and modified membrane (IL-3wt%) as illustrated in Fig. 10. It can be seen that the roughness of the modified membrane surface increases slightly, but the increased rates are only 1.72 % (Ra) and 5.05 % (Rq). In general, inorganic nanoparticles are directly used to modify the roughness of a membrane surface and further increase the contact angle depending on the size effect of the inorganic nanoparticles.[53,54] However, in our experiments, the hydrophobic IL ([Bmim][PF_6]) and PVDF have a high solubility in DMF, and there is no size effect on the membrane surface like inorganic nanoparticles. Therefore, [Bmim][PF_6] has little effect on the roughness of surfaces, which has been proven by AFM. However, the contact angle of the modified membrane increases significantly from 88.1° to 110.1°. Therefore, we can infer that the change of surface energy can remarkably affect the hydrophobicity when the IL has been blended with PVDF in our experiments.[55,56]

Some researchers have prepared different membranes using PVDF as a membrane matrix, whose contact angles have been given. The contact angle of a high-performance PDVF hydrophobic membrane prepared by Zhang et al.[57] is 108.1°, that of a PVDF hydrophobic membrane prepared by Hou et al.[58] is 113°, that of a PVDF-CTFE membrane reported by Zheng et al.[59] is 92.58°, and that of a PVDF-CTFE flat sheet membrane prepared by Wang et al.[60] using a dry-wet phase inversion process is ~108°. In addition, some special inorganic particles have been blended with PVDF and increased the hydrophobicity of the membranes prepared. The contact angels of a $CaCO_3$/PVDF membrane prepared by Hou et al.[54] is 94°, and that of a PVDF membrane blended with calcium stearate is ~110° due to a low adhesion property.[61] However, the contact angle of our modified membranes is 110.1°, which is larger than most of the contact angles displayed in the above literature, indicating that

our PVDF membrane modified by an IL has excellent hydrophobicity. Therefore, the addition of IL can change the hydrophobic effect of PVDF and enhance its hydrophobicity. At the same time, the modified membrane of IL-3wt% has the best hydrophobic effect under our experimental conditions.

IL Leaching

Our modified membranes were prepared by an immersion precipitation process. In order to investigate whether the IL is stably retained in the membranes, IL leaching experiments of the modified membrane were performed both during membrane formation and the exchange of solvent and non-solvent.

The measured conductivity of the DMF was 0 μs cm^{-1}. So the change of conductivity will come from the contribution of IL if IL leaches. In this experiment, the scratched modified membrane was immediately placed into deionized water after the initial conductivity of the deionized water had been recorded. The conductivity of the deionized water with immersed modified membranes was measured every two hours, and this process lasted for 10 days. Over the period of 10 days, the conductivity of deionized water remained unchanged, so we can conclude that the IL is well retained in the PVDF membrane and no leaching occurs during membrane fabrication.

Conclusions

In this work, modified PVDF membranes have been prepared by a non-solvent induced phase inversion by the blending of PVDF with a hydrophobic IL [Bmim][PF_6]. PVDF membranes modified by IL have the best properties in pore size, porosity, and hydrophobicity compared with a pristine PVDF membrane, which can decrease the transport resistance of CO_2 gas and increase CO_2 absorption fluxes in theory. The improvements in membrane properties favour the application of hydrophobic PVDF membranes. The specific experimental conclusions are listed below.

1. The different properties of the modified membranes are characterized as follows. FT-IR spectroscopy indicates that the IL was successfully retained by the PVDF membrane. DSC shows that [Bmim][PF_6] has no significant impact on the melting point and crystallinity degree of the PVDF membrane. TGA reveals the optimum temperature of the modified membrane is below 300°C, otherwise the IL can be pyrolyzed.
2. The addition of IL can influence the structure of the membrane pores due to two competitive actions. The exchange rate of solvent and non-solvent can be influenced by two factors. One is the effect from the hydrogen bond action between IL and DMF, and the other is the effect of the increasing viscosity of the casting solution. The former plays a leading role. The hydrogen bond action between IL and DMF can slow the rate that DMF leaves the membrane during the process of membrane formation. As a result, the pore size of the membrane is enlarged.
3. The addition of IL increases the hydrophobicity of the membrane so that the maximum contact angle is 110.1° in our experiments. The reason is that the fluorine-containing IL is strongly electronegative, making the bond energy of C–F much larger than that of C–H. As a result, PVDF blended with IL has a lower surface energy and leads to the higher hydrophobicity of the modified membranes.
4. The [Bmim][PF_6] is well retained in the PVDF membrane and there is no leaching of IL during membrane fabrication.

Conflicts of Interest

The authors declare no conflicts of interest.

Acknowledgements

The work was supported by Natural Science Foundation of Liaoning Province under Grants 20170540685, and 201402117 and the National Science Foundation of China under Grant 201706163.

References

[1] M. Mehdipour, P. Keshavarz, A. Seraji, S. Masoumi, *Int. J. Greenh. Gas Control* **2014**, *31*, 16. doi:10.1016/J.IJGGC.2014.09.017
[2] R. Naim, A. F. Ismail, T. Matsuura, I. A. Rudaini, S. Abdullah, *RSC Advances* **2018**, *8*, 3556. doi:10.1039/C7RA12045A
[3] M. Saidi, *J. Membr. Sci.* **2017**, *524*, 186. doi:10.1016/J.MEMSCI.2016.11.028
[4] Y. F. Lin, J. W. Kuo, *Chem. Eng. J.* **2016**, *300*, 29. doi:10.1016/J.CEJ.2016.04.119
[5] Y. F. Lin, C. H. Chen, K. L. Tung, T. Y. Wei, S. Y. Lu, K. S. Chang, *ChemSusChem* **2013**, *6*, 437. doi:10.1002/CSSC.201200837
[6] L. Gomez-Coma, A. Garea, J. C. Rouch, T. Savart, J. F. Lahitte, J. C. Remigy, A. Irabien, *J. Membr. Sci.* **2016**, *498*, 218. doi:10.1016/J.MEMSCI.2015.10.023
[7] Y. F. Lin, C. C. Ko, C. H. Chen, K. L. Tung, K. S. Chang, T. W. Chung, *Appl. Energy* **2014**, *129*, 25. doi:10.1016/J.APENERGY.2014.05.001
[8] S. Rajabzadeh, S. Yoshimoto, M. Teramoto, M. Al-Marzouqi, Y. Ohmukai, T. Maruyama, H. Matsuyama, *Separ. Purif. Tech.* **2013**, *108*, 65. doi:10.1016/J.SEPPUR.2013.01.049
[9] Y. F. Lin, W. W. Wang, C. Y. Chang, *J. Mater. Chem.* **2018**, *6*, 9489. doi:10.1039/C8TA00275D
[10] W. T. Xu, Z. P. Zhao, M. Lin, K. C. Chen, *J. Membr. Sci.* **2015**, *491*, 110. doi:10.1016/J.MEMSCI.2015.05.024
[11] C. Y. Huang, C. C. Ko, L. H. Chen, C. T. Huang, K. L. Tung, Y. C. Liao, *Separ. Purif. Tech.* **2018**, *198*, 79. doi:10.1016/J.SEPPUR.2016.12.037
[12] A. L. Ahmad, W. K. W. Ramli, *Separ. Purif. Tech.* **2013**, *103*, 230. doi:10.1016/J.SEPPUR.2012.10.032
[13] R. Wang, H. Y. Zhang, P. H. M. Feron, D. T. Liang, *Separ. Purif. Tech.* **2005**, *46*, 33. doi:10.1016/J.SEPPUR.2005.04.007
[14] S. Rajabzadeh, S. Yoshimoto, M. Teramoto, M. Al-Marzouqi, H. Matsuyama, *Separ. Purif. Tech.* **2009**, *69*, 210. doi:10.1016/J.SEPPUR.2009.07.021
[15] G. D. Kang, Y. M. Cao, *J. Membr. Sci.* **2014**, *463*, 145. doi:10.1016/J.MEMSCI.2014.03.055
[16] S. Sairiam, C. H. Loh, R. Wang, R. Jiraratananon, *J. Appl. Polym. Sci.* **2013**, *130*, 610. doi:10.1002/APP.39197
[17] M. Rahbari-Sisakht, A. F. Ismail, D. Rana, T. Matsuura, *J. Membr. Sci.* **2012**, *415–416*, 221. doi:10.1016/J.MEMSCI.2012.05.002
[18] Y. Zhang, L. Wang, Y. Xu, *Desalination* **2015**, *358*, 84. doi:10.1016/J.DESAL.2014.12.022
[19] A. Razmjou, E. Arifin, G. X. Dong, J. Mansouri, V. Chen, *J. Membr. Sci.* **2012**, *415–416*, 850. doi:10.1016/J.MEMSCI.2012.06.004
[20] S. H. Park, J. H. Kim, S. J. Moon, E. Drioli, Y. M. Lee, *J. Membr. Sci.* **2018**, *550*, 545. doi:10.1016/J.MEMSCI.2017.10.065
[21] J. Albo, A. Irabien, *J. Chem. Technol. Biotechnol.* **2012**, *87*, 1502. doi:10.1002/JCTB.3790
[22] G. Gurau, H. Rodríguez, S. P. Kelley, P. Janiczek, R. S. Kalb, R. D. Rogers, *Angew. Chem.* **2011**, *50*, 12024. doi:10.1002/ANIE.201105198
[23] I. M. Marrucho, L. C. Branco, L. P. N. Rebelo, *Annu. Rev. Chem. Biomol. Eng.* **2014**, *5*, 527. doi:10.1146/ANNUREV-CHEMBIOENG-060713-040024
[24] Z. D. Dai, R. D. Noble, D. L. Gin, X. P. Zhang, L. Y. Deng, *J. Membr. Sci.* **2016**, *497*, 1. doi:10.1016/J.MEMSCI.2015.08.060
[25] R. Shindo, M. Kishida, H. Sawa, T. Kidesaki, S. Sato, S. Kanehashi, K. Nagai, *J. Membr. Sci.* **2014**, *454*, 330. doi:10.1016/J.MEMSCI.2013.12.031
[26] Y. S. Ng, N. S. Jayakumar, M. A. Hashim, *Desalination* **2011**, *278*, 250. doi:10.1016/J.DESAL.2011.05.047

[27] D. S. Lakshmi, S. Santoro, E. Avruscio, A. Tagarelli, A. Figoli, *Int. J. Membr. Sci. Technol.* **2015**, *2*, 65. doi:10.15379/2410-1869.2015.02.02.07
[28] H. R. Mahdavi, N. Azizi, M. Arzani, T. Mohammadi, *J. Nat. Gas Sci. Eng.* **2017**, *46*, 275. doi:10.1016/J.JNGSE.2017.07.024
[29] A. A. Akhmetshina, I. M. Davletbaeva, E. S. Grebenschikova, T. S. Sazanova, A. N. Petukhov, A. A. Atlaskin, E. N. Razov, I. I. Zaripov, C. F. Martins, L. A. Neves, I. V. Vorotyntsev, *Membranes* **2015**, *6*, 4. doi:10.3390/MEMBRANES6010004
[30] S. K. Chaurasia, R. K. Singh, S. Chandra, *CrystEngComm* **2013**, *15*, 6022. doi:10.1039/C3CE40576A
[31] B. Lin, G. Qiao, F. Q. Chu, S. Zhang, N. Y. Yuan, J. N. Ding, *RSC Adv.* **2017**, *7*, 1056. doi:10.1039/C6RA25460H
[32] S. Awasthi, V. Kiran, B. Gaur, *Int. J. Hydrogen Energy* **2017**, *42*, 11710. doi:10.1016/J.IJHYDENE.2017.03.018
[33] S. Al-Gharabli, W. Kujawski, Z. A. El-Rub, E. M. Hamad, J. Kujawa, *J. Membr. Sci.* **2018**, *556*, 214. doi:10.1016/J.MEMSCI.2018.04.012
[34] P. G. Saiz, A. C. Lopes, S. E. Barker, R. F. de Luis, M. I. Arriortua, *Mater. Des.* **2018**, *155*, 325. doi:10.1016/J.MATDES.2018.06.013
[35] X. S. Lin, Q. Wen, Z. L. Huang, Y. Z. Cai, P. J. Halling, Z. Yang, *Process Biochem.* **2015**, *50*, 1852. doi:10.1016/J.PROCBIO.2015.07.019
[36] K. Li, J. F. Kong, D. L. Wang, W. K. Teo, *AIChE J.* **1999**, *45*, 1211. doi:10.1002/AIC.690450607
[37] G. Rashinkar, R. Salunkhe, *J. Mol. Catal. Chem.* **2010**, *316*, 146. doi:10.1016/J.MOLCATA.2009.10.013
[38] R. Kurane, V. Gaikwad, J. Jadhav, R. Salunkhe, G. Rashinkar, *Tetrahedron Lett.* **2012**, *53*, 6361. doi:10.1016/J.TETLET.2012.09.021
[39] A. Pinkert, K. N. Marsh, S. S. Pang, M. P. Staiger, *Chem. Rev.* **2009**, *109*, 6712. doi:10.1021/CR9001947
[40] A. K. Gupta, R. Bajpai, J. M. Keller, *J. Polym. Res.* **2008**, *15*, 275. doi:10.1007/S10965-007-9168-9
[41] Z. Z. Yang, Y. N. Zhao, L. N. He, *RSC Adv.* **2011**, *1*, 545. doi:10.1039/C1RA00307K
[42] A. H. Jadhav, G. M. Thorat, K. Lee, A. C. Lim, H. Kang, J. G. Seo, *Catal. Today* **2016**, *265*, 56. doi:10.1016/J.CATTOD.2015.09.048
[43] P. Attri, P. M. Reddy, P. Venkatesu, *J. Phys. Chem. B* **2010**, *114*, 6126. doi:10.1021/JP101209J
[44] R. Matz, *Desalination* **1972**, *10*, 1. doi:10.1016/S0011-9164(00)80243-X
[45] H. Strathmann, K. Kock, P. Amar, R. W. Baker, *Desalination* **1975**, *16*, 179. doi:10.1016/S0011-9164(00)82092-5
[46] L. Broens, F. W. Altena, C. A. Smolders, D. M. Koenhen, *Desalination* **1980**, *32*, 33. doi:10.1016/S0011-9164(00)86004-X
[47] C. A. Smolders, A. J. Reuvers, R. M. Boom, I. M. Wienk, *J. Membr. Sci.* **1992**, *73*, 259. doi:10.1016/0376-7388(92)80134-6
[48] N. A. A. Sani, W. J. Lau, A. F. Ismail, *J. Polym. Eng.* **2014**, *34*, 489. doi:10.1515/POLYENG-2014-0038
[49] M. Rezaei, A. F. Ismail, Gh. Bakeri, S. A. Hashemifard, T. Matsuura, *Chem. Eng. J.* **2015**, *260*, 875. doi:10.1016/J.CEJ.2014.09.027
[50] D. Ghoshdastidar, D. Ghosh, S. Senapati, *J. Phys. Chem. B* **2016**, *120*, 492. doi:10.1021/ACS.JPCB.5B07179
[51] S. Wongchitphimon, R. Wang, R. Jiraratananon, *J. Membr. Sci.* **2011**, *381*, 183. doi:10.1016/J.MEMSCI.2011.07.022
[52] M. Rezaei, A. F. Ismail, S. A. Hashemifard, Gh. Bakeri, T. Matsuura, *Int. J. Greenh. Gas Control* **2014**, *26*, 147. doi:10.1016/J.IJGGC.2014.04.021
[53] P. G. Jin, C. Huang, J. X. Li, Y. D. Shen, L. Wang, *R. Soc. Open Sci.* **2017**, *4*, 171321. doi:10.1098/RSOS.171321
[54] D. Y. Hou, G. H. Dai, H. Fan, J. Wang, C. W. Zhao, H. J. Huang, *Desalination* **2014**, *347*, 25. doi:10.1016/J.DESAL.2014.05.028
[55] H. Lei, M. N. Xiong, J. Xiao, L. P. Zheng, Y. R. Zhu, X. X. Li, Q. X. Zhuang, Z. W. Han, *Prog. Org. Coat.* **2017**, *103*, 182. doi:10.1016/J.PORGCOAT.2016.10.036
[56] J. Gao, X. Xu, C. Fan, X. Wang, Y. Dai, X. Liu, *Mater. Lett.* **2014**, *121*, 219. doi:10.1016/J.MATLET.2014.01.149
[57] H. Zhang, X. L. Lu, Z. Y. Liu, Z. Ma, S. Wu, Z. D. Li, X. Kong, J. J. Liu, C. R. Wu, *J. Membr. Sci.* **2018**, *550*, 9. doi:10.1016/J.MEMSCI.2017.12.059
[58] D. Y. Hou, J. Wang, D. Qu, Z. K. Luan, C. W. Zhao, X. J. Ren, *Water Sci. Technol.* **2009**, *59*, 1219. doi:10.2166/WST.2009.080
[59] L. B. Zheng, J. Wang, Y. S. Wei, Y. Zhang, K. Li, Z. J. Wu, *RSC Adv.* **2016**, *6*, 20926. doi:10.1039/C5RA28081H
[60] J. Wang, L. B. Zhang, Z. J. Wu, Y. Zhang, X. H. Zhang, *J. Membr. Sci.* **2016**, *497*, 183. doi:10.1016/J.MEMSCI.2015.09.024
[61] K. Ekambaram, M. Doraisamy, *Desalination* **2016**, *385*, 24. doi:10.1016/J.DESAL.2016.01.029